Available online at www.sciencedirect.com
ScienceDirect
Dyes and Pigments 77 (2008) 303–314
DYES and PIGMENTS
www.elsevier.com/locate/dyepig

Molecular aggregation in Langmuir–Blodgett films of azo dye/liquid crystal mixtures

K. Inglot, A. Kaleta, T. Martyński, D. Bauman*

Faculty of Technical Physics, Poznań University of Technology, Nieszawska 13A, 60-965 Poznań, Poland

Received 8 May 2007; received in revised form 22 May 2007; accepted 22 May 2007
Available online 8 June 2007

Abstract

Studies of azo dye/liquid crystal mixtures in monolayers formed at an air–water interface (Langmuir films) and on a solid surface (Langmuir–Blodgett films) were performed. Six azo dyes with various molecular structures and two liquid crystal materials: 4-octyl-4′-cyanobiphenyl (8CB) and *trans*-4-octyl(4′-cyanophenyl)-cyclohexane (8PCH) were used. The dyes were added to the liquid crystal matrices at various concentrations and the surface pressure–mean molecular area isotherms for the resultant Langmuir films were recorded. On the basis of the isotherm runs, conclusions concerning the molecular organization and the miscibility of the components in the ultrathin films were drawn. Absorption spectra for the Langmuir–Blodgett films, using both natural and linearly polarized light were recorded. Information regarding intermolecular interactions in the mixtures of the nonamphiphilic dye and the liquid crystal, with the polar terminal group was obtained. The ability of dye molecules to form self-aggregates at the air–solid substrate interface was observed. The influence of the molecular structure and the concentration of a dye on aggregates' geometry is discussed. It was found that at low dye concentrations in the liquid crystal J-type aggregates are formed. High dye contents are conducive to the creation of H-type aggregation, which improve the molecular packing in the Langmuir–Blodgett film.

Keywords: Langmuir film; Langmuir–Blodgett film; Azo dye; Liquid crystal; Electronic absorption; Molecular aggregate

1. Introduction

In recent years, much interest has been directed to molecular organic materials in which aggregation phenomena occur. Such systems display intriguing optical properties and can find application as novel functional materials for molecular electronics and photonics. In particular, it is known that the formation of molecular aggregates has a strong effect on the design and molecular properties of systems that contain species having sizes on the nanoscale. One of the methods used in the fabrication of nanosystems is the Langmuir–Blodgett (LB) technique [1–3]. In films formed using this technique, molecules are in a highly ordered environment, similar to those in solid matrices, where aggregation of aromatic molecules is frequently observed [4].

In this paper we report the study of the aggregation properties of some azo dyes in LB films. Azo dyes are known as compounds whose molecules have a tendency towards aggregation, in the ground electronic state [4–6] itself. Because of large change of the dipole moment at π → π* transition, these molecules are characterized by a high value of hyperpolarizability and therefore, when they are incorporated into highly oriented matrices, can find application in nonlinear optics systems [7].

The molecular aggregation and orientation in LB films are inherently dependent upon the molecular organization in spread monolayers on the water surface (Langmuir films). Investigations carried out previously in our laboratory had indicated that azo dye molecules are not able to form stable and compressible Langmuir films [8,9]. In such a case it is

---

* Corresponding author. Tel.: +48616653172; fax: +48616653164.
E-mail address: bauman@phys.put.poznan.pl (D. Bauman).

0143-7208/$ - see front matter © 2007 Elsevier Ltd. All rights reserved.
doi:10.1016/j.dyepig.2007.05.016

necessary to use the admixture of a compound that is able to make stable monolayers at the interfaces and can act as a supporting matrix. Two liquid crystals: 4-octyl-4′-cyanobiphenyl (8CB) and *trans*-4-octyl(4′-cyanophenyl)-cyclohexane (8PCH) were used. These two liquid crystals are known to form homogeneous Langmuir and LB films under appropriate circumstances [10–13].

2. Materials and methods

The molecular structure of the dyes used are presented in Table 1. Fig. 1 shows the normalized absorption spectra of the chosen dyes, dissolved in ethanol, in the visible spectral region. All of the dyes were synthesized and chromatographically purified in the Institute of Dyes at Łódź University of Technology, Poland.

The liquid crystals 4-octyl-4′-cyanobiphenyl (8CB) and *trans*-4-octyl(4′-cyanophenyl)-cyclohexane (8PCH) were purchased from the Dąbrowski Laboratory at the Military University of Technology, Warsaw (Poland) and were used without further purification.

Spectroscopic grade chloroform was used to prepare the spreading solutions. The dye–liquid crystal mixture solutions were made at a constant concentration of 8CB or 8PCH (0.3 g/dm^3) with appropriate amounts of the dye, in order to obtain the molar fraction (MF) of the dye in the whole range of possible concentrations (depending on the dye solubility). The solution was then spread onto the deionized water subphase to form a monolayer that was equilibrated for about 15 min to allow the chloroform to evaporate. The surface pressure was measured as a function of the area using a Wilhelmy plate balance (Minitrough 2 Langmuir–Blodgett system, KSV Instruments Ltd., Finland). The experiments were performed at a subphase temperature of (20.5 ± 0.5) °C. Further experimental information concerning Langmuir film preparation is given elsewhere [14].

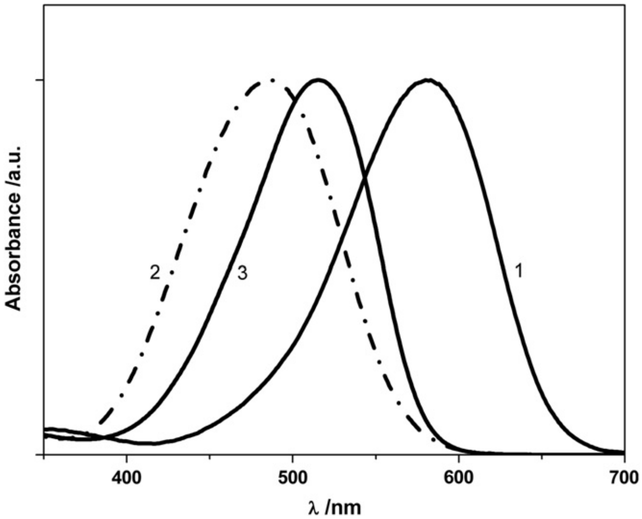

Fig. 1. Normalized absorption spectra of dyes **1** (1), **3** (2) and **6** (3) dissolved in ethanol (MF = 1.5×10^{-7}).

Table 1
Molecular structure of azo dyes investigated

Dye code	Molecular structure
1	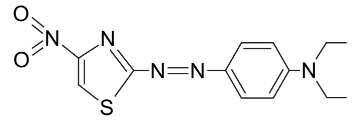
2	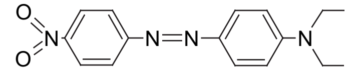
3	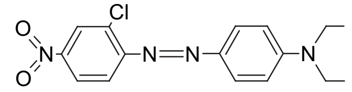
4	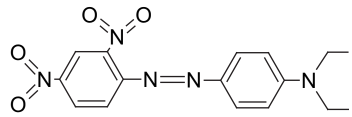
5	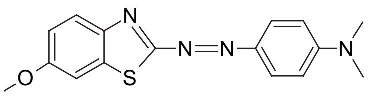
6	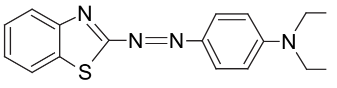

Polished quartz plates ($35 \times 10 \times 1$ mm^3) were used as solid substrates that possessed a hydrophilic surface suitable for LB film fabrication. The substrates were dipped and raised through the floating layer vertically at a speed of 5 mm/min at a constant surface pressure. The dipping stroke was 25 mm. The deposition of the film onto the quartz was successful only on raising the substrate. Repeated attempts to transfer a floating layer onto quartz slides failed. Therefore, only one dipping and one raising were made. The transfer ratio TR, defined as the ratio of the actual decrease in the subphase area to the actual area on the substrate that was coated by the floating layer, was estimated to be between 1.0 and 1.2.

The absorption spectra of LB films were recorded in the UV–vis region using natural and linearly polarized light by means of a spectrophotometer CARY 400, equipped with an angular sample holder. Glan-Thompson polarizers were used to obtain polarized incident light.

In order to analyze the absorption spectra over a wide range of dye concentrations, some additional measurements for dyes that were dissolved in 8CB were performed in sandwich cells made of two glass plates separated by the spacer of 10 μm in thickness. Such cells allowed the recording of the absorption spectra of dye/8CB mixtures at MF from 10^{-3} to 10^{-2}.

3. Results and discussion

3.1. Surface pressure–mean molecular area isotherm

After spreading solutions of the azo dyes at the water surface in the trough, large patches of the dye on the water were observed. Also the surface pressure did not rise during the compression process. Thus, none of the azo dyes under investigation can produce stable and compressible monolayer. However, when the dyes were mixed with 8CB or with 8PCH at appropriate concentrations, compression was possible and stable monolayers at the air–water interface were obtained.

Figs. 2 and 3 present surface pressure–mean molecular area ($\pi-\Sigma$) isotherms of Langmuir films of pure liquid crystals and of **5**/8CB and **3**/8PCH mixtures, as examples. The isotherms were recorded up to the molar fraction of the dye at which, just after spreading, microcrystallites in the chloroform solution were not visible to the naked eye. For the compounds investigated, the isotherms were recorded both during compression and during expansion processes. Only small differences in the isotherm runs were found. This means that the equilibrium conditions were obtained.

The $\pi-\Sigma$ runs for the pure liquid crystals, 8CB and 8PCH, are in agreement with those given in literature [10–13]. The increase in π begins at the area equal to Σ_0 being the first edge of the phase transition. This indicates the formation of the condensed monolayer, which collapses at the area Σ_C and the surface pressure π_C. The collapse point is recognized as the point in the isotherm where the ratio $\partial\pi/\partial\Sigma$ begins to decrease due to the next phase transition. The characteristic values of $\pi-\Sigma$ isotherms for Langmuir films of pure liquid crystals and dye/liquid crystal mixtures with various MF are presented in Tables 2 and 3. The following data are presented: Σ_{ext} – the value of the area obtained by extrapolating the tangent of the tilt angle of the $\pi-\Sigma$ plot (the part representing the condensed monolayer creation) to $\pi = 0$ (see insert in Fig. 2), Σ_C – the value of the collapse area and π_C – the value of the collapse pressure.

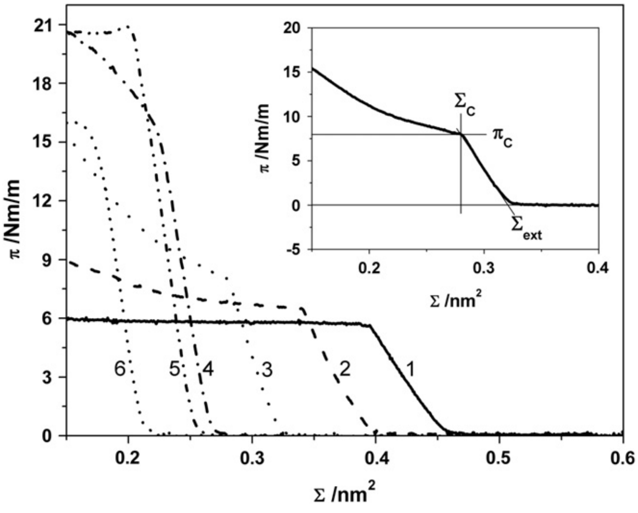

Fig. 2. Surface pressure–mean molecular area isotherms of Langmuir films of pure 8CB (1) and of binary mixtures of dye **5** in 8CB with MF of 0.1 (2), 0.2 (3), 0.3 (4), 0.4 (5) and 0.5 (6).

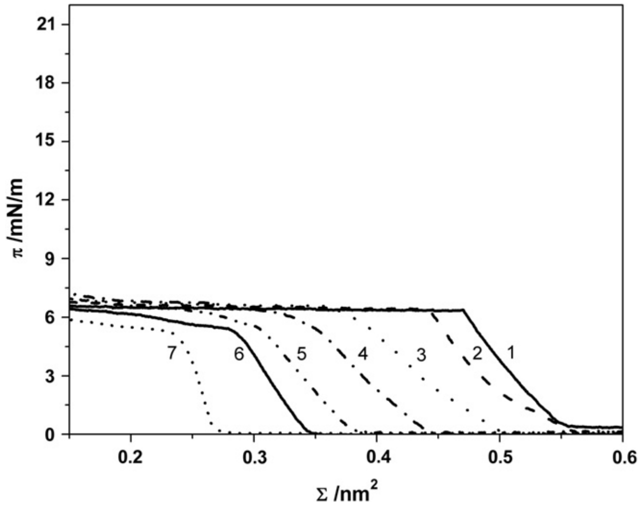

Fig. 3. Surface pressure–mean molecular area isotherms of Langmuir films of pure 8PCH (1) and of binary mixtures of dye **3** in 8PCH with MF of 0.1 (2), 0.2 (3), 0.3 (4), 0.4 (5), 0.5 (6) and 0.6 (7).

Table 2
Values of the area per molecule, the collapse pressure and the average angle between the normal to the water surface and rigid molecular cores for azo dyes mixed with 8CB

Compound	MF of dye	Σ_{ext} (nm^2)	Σ_C (nm^2)	π_C (mN m^{-1})	φ_{av} (°)
8CB	–	0.46	0.41	4.8	61
1/8CB	0.1	0.36	0.29	6.1	37
	0.2	0.27	0.24	8.5	29
	0.3	0.22	0.20	19.0	23
	0.4	0.20	0.18	24.0	20
	0.5	0.16	0.14	15.7	15
2/8CB	0.1	0.34	0.30	7.2	38
	0.2	0.30	0.26	8.8	31
	0.3	0.29	0.27	13.0	31
	0.4	0.27	0.25	16.4	28
	0.5	0.29	0.28	12.4	30
3/8CB	0.1	0.36	0.31	6.0	39
	0.2	0.28	0.24	7.0	28
	0.3	0.23	0.17	21.0	18
	0.4	0.22	0.20	22.0	21
	0.5	0.22	0.20	19.0	20
4/8CB	0.1	0.39	0.35	6.5	39
	0.2	0.31	0.26	6.8	28
	0.3	0.32	0.27	6.5	29
	0.4	0.24	0.21	6.5	21
	0.5	0.22	0.20	5.9	18
5/8CB	0.1	0.39	0.34	6.5	43
	0.2	0.32	0.28	7.8	32
	0.3	0.27	0.22	15.4	23
	0.4	0.25	0.20	20.9	20
	0.5	0.21	0.17	15.4	16
6/8CB	0.1	0.39	0.34	6.0	47
	0.2	0.32	0.28	8.0	39
	0.3	0.26	0.21	24.0	28
	0.4	0.25	0.20	23.5	28
	0.5	0.20	0.16	23.9	23

Table 3
Values of the area per molecule, the collapse pressure and the average angle between the normal to the water surface and rigid molecular cores for azo dyes mixed with 8PCH

Compound	MF of dye	Σ_{ext} (nm^2)	Σ_{C} (nm^2)	π_{C} (mN m^{-1})	φ_{av} (°)
8PCH	–	0.56	0.48	5.3	54
1/8PCH	0.1	0.52	0.45	6.3	51
	0.2	0.37	0.31	6.1	32
	0.3	0.33	0.23	16.0	23
	0.4	0.23	0.16	16.9	16
	0.5	0.21	0.17	15.7	17
2/8PCH	0.1	0.56	0.49	6.4	42
	0.2	0.47	0.39	6.7	41
	0.3	0.39	0.32	7.9	32
	0.4	0.35	0.30	10.5	30
	0.5	0.30	0.25	11.5	24
	0.6	0.27	0.25	6.6	24
3/8PCH	0.1	0.52	0.45	6.6	49
	0.2	0.49	0.37	6.7	38
	0.3	0.44	0.34	6.0	33
	0.4	0.38	0.30	5.6	28
	0.5	0.34	0.27	5.2	27
	0.6	0.27	0.24	5.1	21
4/8PCH	0.1	0.49	0.43	5.8	46
	0.2	0.56	0.49	5.8	52
	0.3	0.45	0.40	5.9	39
	0.4	0.33	0.28	6.1	25
	0.5	0.30	0.26	5.9	24
	0.6	0.25	0.22	5.5	20
5/8PCH	0.1	0.50	0.41	6.2	43
	0.2	0.40	0.34	6.6	33
	0.3	0.32	0.26	7.7	24
	0.4	0.29	0.23	16.0	20
	0.5	0.29	0.23	6.5	20
6/8PCH	0.1	0.47	0.39	5.7	44
	0.2	0.40	0.33	6.3	38
	0.3	0.26	0.20	18.0	23
	0.4	0.24	0.21	25.9	25
	0.5	0.22	0.18	21.8	22

The values of the areas found from the isotherms suggest that, in the monolayer formed of all compounds, the rigid cores of the molecules must be tilted with respect to the water surface. Assuming that the mean molecular area in the Langmuir film is determined by the rigid core of the molecule and taking the experimental Σ value into account, it is possible to calculate the tilt angle. The tilt angle φ for 8CB and 8PCH, given in Tables 2 and 3, was estimated as the angle between the long axis of the rigid core of liquid crystal molecules and the normal to the water surface in the vicinity of the collapse point. The findings are in agreement with the data given in literature [10,13,15]. Knowing additionally the area of each dye molecule and taking into account the mixture composition, estimation of the average angles φ_{av} for mixed Langmuir films became possible. The appropriate values are presented in Tables 2 and 3 too.

From the analysis of the isotherm shapes and the data given in Tables 2 and 3, it follows that azo dyes at the appropriate concentration influence strongly the alignment and the packing of the liquid crystal molecules at the air–water interface. The molecules of both 8CB and 8PCH are tilted at a very large angle with respect to the normal to the water surface and, therefore, monolayers formed from them are unstable. The addition of the dye increases the packing density of liquid crystal molecules and, as a result, the angle φ_{av} decreases. Simultaneously the rigidity and the stability of the Langmuir films increase, as is confirmed by the rise of the isotherm steepness and the value of π_{C}. For the most dyes, characteristic dye concentration is at MF = 0.4. At such a content of the dye, both the tilt angle of the π–Σ plot and π_{C} have their highest values. These observations indicate that dye molecules were able to 'stiffen' the molecules of liquid crystals under investigation. As the MF of the dye increases further, the π_{C} value decreases, indicating that the monolayer stability becomes smaller. When the content of a dye is higher than that of 8CB or 8PCH, the liquid crystal cannot play further the role of a host. Although compression is still possible, in the most cases the average area per molecule is too small for even the most dense packing of molecules in a monolayer, which suggests the creation of three-dimensional (3D) groups. Comparing the results gathered in Table 2 with those in Table 3 it is seen that all of the effects mentioned above depend to some extent on the kind of the liquid crystal. The influence of the molecular structure of the dyes on the behaviour of azo dye/liquid crystal monolayers at the water surface is also clearly seen.

The miscibility or the phase separation of the two components of the Langmuir film can be determined on the basis of the shape of π–Σ isotherms for various MFs, using the excess criterion and the surface phase rule [16]. Let us define the excess of the average area per molecule, Σ_{E}, at given surface pressure, as follows:

$$\Sigma_{\text{E}} = \Sigma_{12} - (x_1\Sigma_1 + x_2\Sigma_2) \tag{1}$$

Here, Σ_{12} is the average molecular area in the two component film. x_1 and x_2 are the mole fractions of the components, and Σ_1 and Σ_2 are the single component areas at the same π value.

If Σ_{E} is equal to zero, the average area per molecule follows the additivity rule, $\Sigma_{12} = x_1\Sigma_1 + x_2\Sigma_2$, which means that, in the mixture, ideal mixing or complete immiscibility occurs. Deviation from zero, either positive or negative, indicates miscibility and non-ideal behaviour. The excess area per molecule for dye/liquid crystal mixtures in Langmuir films, at the surface pressure $\pi = 3$ mN/m is plotted in Figs. 4 and 5, as a function of MF of the dye. The noticeable deviation from the additivity rule is observed. For dyes **1**, **5** and **6** mixed with both liquid crystals this deviation is predominantly negative meaning a contraction of the two component films due to attractive interactions among dye and liquid crystal molecules [16,17]. In the case of other dyes the deviation is mostly negative for their mixtures with 8CB, and positive when they are mixed with 8PCH. This indicates that the cyclohexane ring present in the 8PCH molecule can cause the occurrence of repulsive interactions.

The values of $\Sigma_{\text{E}} \neq 0$ for all binary mixtures investigated would suggest that two components in Langmuir films are always well miscible. However, the information from the surface phase rule [16] should be additionally taken into

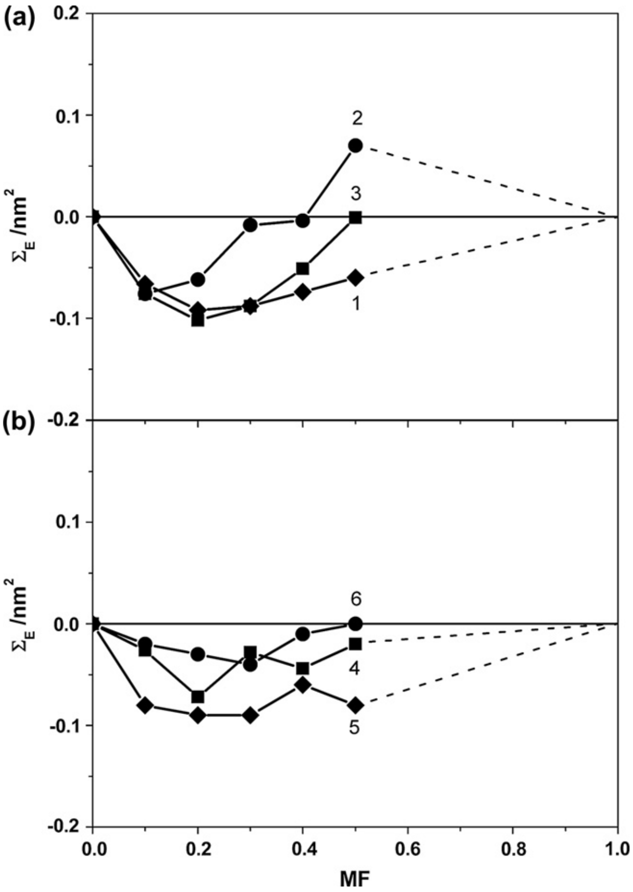

Fig. 4. Plot of the excess of the mean molecular area per molecule, Σ_E, of **1–6** mixed with 8CB versus MF of a dye at $\pi = 3$ mN/m: **1** (1), **2** (2), **3** (3), **4** (4) **5** (5) and **6** (6).

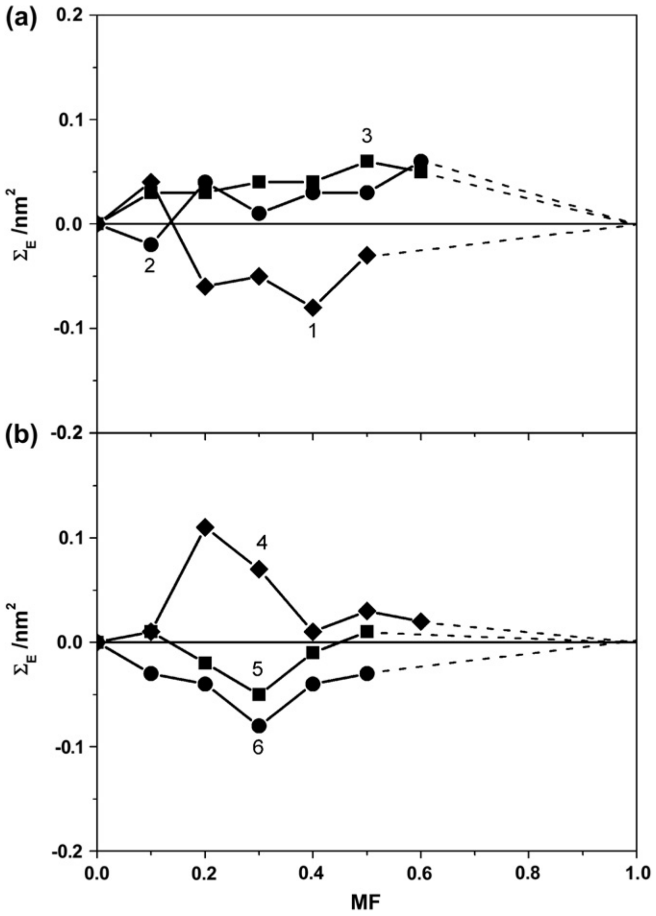

Fig. 5. Plot of the excess of the mean molecular area per molecule, Σ_E, of **1–6** mixed with 8PCH versus MF of a dye at $\pi = 3$ mN/m: **1** (1), **2** (2), **3** (3), **4** (4) **5** (5) and **6** (6).

account. This rule states that if components are miscible, the π_C value should change with the mixture composition. Thus, the dependence of the π_C value on the composition of Langmuir films that are formed from dye/liquid crystal mixtures, seen in Tables 2 and 3, indicates that in the case of **4**/8CB, **3**/8PCH and **4**/8PCH mixtures the immiscibility or at least only partial miscibility of dye and liquid crystal molecules can be postulated. This results from the fact that although the additivity rule is not fulfilled, π_C remains constant.

3.2. Electronic absorption spectra

The Langmuir–Blodgett films of the dye/liquid crystal mixtures were obtained after deposition of the floating monolayer on quartz slides at a surface pressure below the collapse point, i.e., during formation of the homogeneous condensed monolayer on the water surface.

Fig. 6 presents normalized long wavelength absorption spectra of all of the azo dyes under investigation mixed with 8CB and with 8PCH (MF = 0.5) in LB films. The MF of dye **3** in 8CB was exceptionally 0.2, because at higher MFs of this dye it was not possible to obtain LB films with a reliable transfer ratio. For comparison, the dyes were also dissolved in 8CB at MF = 10^{-2} and measured in a sandwich cell. Fig. 7 shows absorption spectra of dye **2** mixed with 8CB (Fig. 7a) and with 8PCH (Fig. 7b) at various MFs. The characteristic parameters of the absorption spectra of LB films of all the dye/liquid crystal mixtures under investigation are presented in Table 4. The data for dye/8CB mixtures measured in sandwich cell at MF = 10^{-2} and in ethanol at MF = 1.5×10^{-7} are also given in this table. The absorption spectra of dyes **1–6** in 8CB in the sandwich cell are very similar in shape to those for the dyes in ethanol. The differences in the maximum position and the half-bandwidth value may be attributed to the differing values of the refractive index and dielectric constant of both solvents. However, a significant difference in the shape of the absorption band of all the dyes in the LB films, with respect to those in the sandwich cell (at 50-fold lower concentration), is observed. The spectra are strongly broadened and mostly red-shifted (for dye **1** at each concentration two maxima or a maximum with distinct shoulder in 8PCH at higher MF can be distinguished). Moreover, the absorption intensity does not vary proportionally to the MF of a dye in the liquid crystal (see Fig. 7). All these effects suggest the creation of some types of self-aggregates among the dye molecules in LB films, in the ground state.

It is well established that if sufficiently strong electronic transitions in molecules exist, the exciton splitting of excited

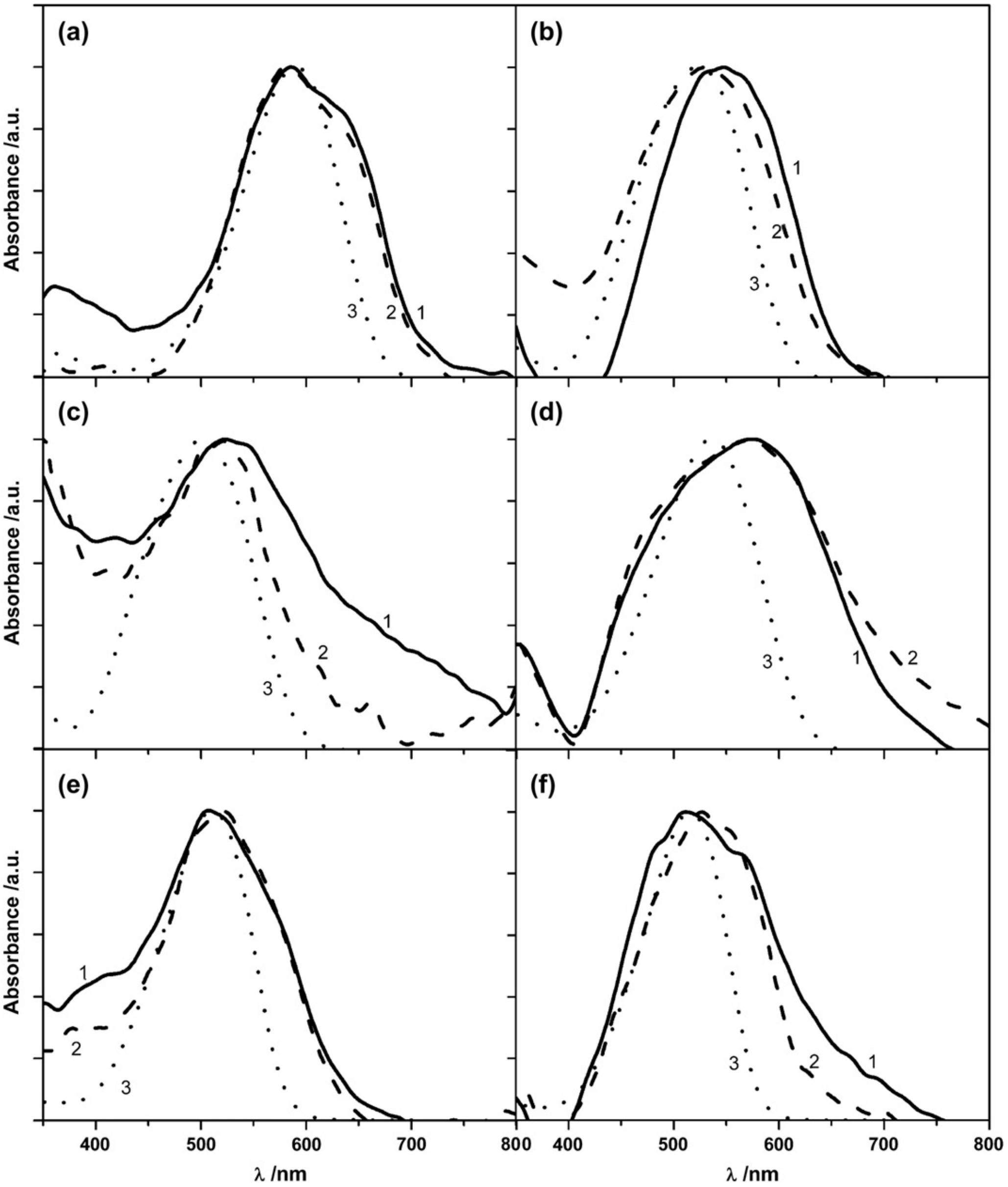

Fig. 6. Longwavelength absorption spectra of dyes **1–6** mixed with 8CB (1) and 8PCH (2) in LB film (MF = 0.2 for **3** and 0.5 for other dyes) and with 8CB in sandwich cell (MF = 10^{-2}): (a) dye **1**, (b) dye **2**, (c) dye **3**, (d) dye **4**, (e) dye **5**, and (f) dye **6**.

states may be observed in molecular aggregates [18,19]. The molar extinction coefficient of dyes **1–6** is quite large at over 20,000. Thus the exciton coupling is most likely to occur in LB films.

Molecular exciton coupling theory [18] predicts that in the simplest case of a two molecule system, the dipole–dipole interactions result in splitting the energy level of the excited state into two levels with higher and lower energies relative to the undisturbed excited state. The change in energies of these two levels is Davydov splitting and can be calculated from the equation:

$$\Delta E = E'' - E' = 2 \cdot \left(\frac{M_i \cdot M_j}{R_{ij}^3} - 3 \frac{(M_i \cdot R_i)(M_j \cdot R_j)}{R_{ij}^5} \right) \tag{2}$$

Here, M_i and M_j are the electric dipole transition moments in molecules i and j, respectively, and R_{ij} is the centre to centre distance between these molecules.

In the case of the co-planar alignment of the dipole transition moments of two molecules, the transition to one of the excited states, corresponding to the antiparallel arrangement of dipole moments is forbidden. The energy difference between the excited monomer level and the exciton level, $\Delta\varepsilon$, is given by [18]:

$$\Delta\varepsilon = \frac{1}{2}\Delta E = \frac{M^2}{R_{ij}^3}\left(1 - 3\cos^2\theta\right) \tag{3}$$

Here, θ is the angle between the transition moment direction and the line connecting the molecules' centres. When

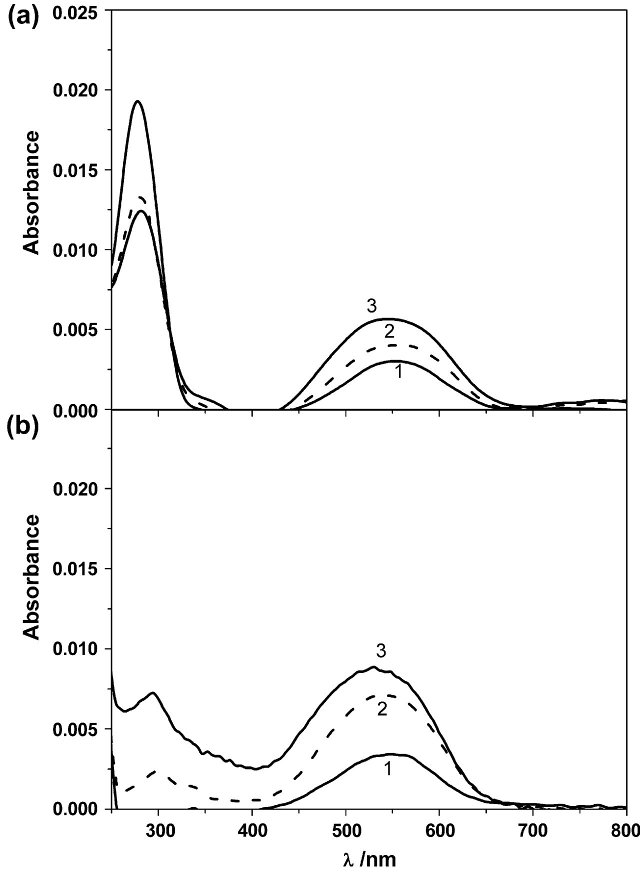

Fig. 7. Absorption spectra of LB films formed of **2**/liquid crystal mixtures with MF of a dye of 0.1 (1), 0.3 (2) and 0.5 (3) for: (a) **2**/8CB and (b) **2**/8PCH mixtures.

$0° \leq \theta < 54.7°$, the exciton level is energetically located below the monomer level causing a red shift in the electronic absorption spectrum, creating aggregates termed J-aggregates [20]. For $54.7° < \theta \leq 90°$, the exciton level is located energetically above the monomer level, causing a blue shift. Corresponding aggregates are called H-aggregates [20]. When $\theta \approx 54.7°$, no shift in the absorption spectrum is observed. The aggregates are then termed I-aggregates [21].

Following the results presented in Table 4, at low concentrations of the dye in LB films, the absorption maximum position shifts towards longer wavelengths (up to .50 nm) with respect to the wavelength of the dye in the sandwich cell. Upon increasing MF, the wavelength of the maximum band shortens. Indeed, significant differences in the change of the absorption band shape (λ and δ), at the same dye content in a liquid crystal, for various dyes occur. This indicates the influence of the molecular structure of the substituents on the spectral properties of the dyes under investigation. The above mentioned behaviour is noticed for the maximum position for all the mixtures. Thus, it can be suggested that with the change of the dye concentration in the LB films, various kinds of aggregates are formed. One of the possibilities is assumption that, at low MFs, some fraction of J-aggregates is created, whereas at higher MFs the H-aggregates appear too. For this reason an attempt was made to separate the longwavelength absorption spectra for the dye/liquid crystal mixtures under investigation into two or three bands, corresponding to the absorption of monomers, J- and/or H-dimers. It was supposed that at $MF = 10^{-2}$, the dye molecules would occur only in their monomeric form. Thus, the values of λ and δ for the monomer (M) absorption band were taken from the measurements in the sandwich cell. Next, one or two additional

Table 4
The position of absorption maximum, λ_{max}, and the half-bandwidth of the longwavelength absorption band, δ, of azo dye dissolved in ethanol and azo dye/liquid crystal mixtures investigated in sandwich cells and in LB films

Mixture	Dye											
	1		**2**		**3**		**4**		**5**		**6**	
	λ_{max} (nm)	δ (cm^{-1})	λ_{max} (nm)	δ (cm^{-1})	λ_{max} (nm)	δ (cm^{-1})	λ_{max} (nm)	δ (cm^{-1})	λ_{max} (nm)	δ (cm^{-1})	λ_{max} (nm)	δ (cm^{-1})
Dye/ethanol												
$MF = 1.5 \times 10^{-7}$	580	3210	508	4530	486	4720	512	4470	511	4025	515	3627
Sandwich cell dye/8CB												
$MF = 10^{-2}$	590	3190	524	4170	503	4860	537	4140	508	4300	517	4010
LB dye/8CB												
MF = 0.1	593,638	3060	570	5280	537	5420	579	5560	524	4170	537	3730
MF = 0.2	601,643	3700	570	5340	518	5830	589	4720	524	4150	517	3990
MF = 0.3	598,637	3890	560	5560	–[a]	–[a]	598	5690	509	4420	511	4530
MF = 0.4	590,640	3730	550	5710	–[a]	–[a]	591	6810	509	4790	511	4720
MF = 0.5	593,641	3980	543	5830	–[a]	–[a]	575	6940	509	5050	512	6110
LB dye/8PCH												
MF = 0.1	587,633	3330	551	4220	522	4750	–[b]	–[b]	526	4230	535	3510
MF = 0.2	590,635	3550	550	4380	523	4800	550	6090	512	4460	528	3900
MF = 0.3	590,635	4170	544	5100	524	4970	555	7260	506	4590	523	4350
MF = 0.4	580,635	4250	540	5370	523	5090	578	7400	499	4800	524	4640
MF = 0.5	583,635	4540	533	5880	524	5140	567	8240	501	4920	528	4810

[a] Transfer impossible.
[b] Absorbance not measurable.

maxima were assumed, which should appear at the longer (J-dimer) and shorter (H-dimer) wavelengths with respect to the peak position of the monomer. A sum of normalized Gaussians was used as a model function for the experimentally obtained absorption band of dye/liquid crystal mixtures in LB films.

In Figs. 8 and 9, the exemplary decomposition of the absorption band into Gaussian-type components for **4**/8CB and **2**/8PCH mixtures, respectively, at MF = 0.1 (a) and 0.5 (b) are shown. In Tables 5 and 6, some values that are characteristic for component bands are presented. Following are the data resulting from the best fits : the wavenumbers of peak positions, $\bar{\nu}_{\mathrm{M}}$, $\bar{\nu}_{\mathrm{H}}$ and $\bar{\nu}_{\mathrm{J}}$, as well as the ratios of the appropriate bands integral absorptions, $A_{\mathrm{H}}/A_{\mathrm{M}}$, $A_{\mathrm{J}}/A_{\mathrm{M}}$ and $A_{\mathrm{H}}/A_{\mathrm{J}}$. The data are given for MF = 0.1, 0.3 and 0.5 (for **6**/8CB mixtures MF = 0.2 and 0.4 were considered too). Additionally, for all the dye/liquid crystal mixtures at MF = 0.5 and for some mixtures at MF = 0.3, the attempt of the decomposition the absorption spectra into two components attributed to the absorption of J- and H-dimers were made.

It should be noticed that the data listed in Tables 5 and 6 can be treated only qualitatively and not quantitatively. This is because the simplest models were taken into account here. Namely, it was assumed that only one kind of J- or H-dimer is created, in which the angle θ between the transition moment direction and the line connecting the molecules' centres in the dimer is the same. Meanwhile, it is highly probable that a broad distribution of structurally different dimers is formed, leading to a simultaneous presence of a slightly red- and blue-shifted absorptions. Thus, different positions of J-bands and H-bands maxima at various MFs (Tables 5 and 6), are observed. Moreover, it was assumed that the co-planar alignment of the dipole moment transitions occured in the dimer. As an alternative, a dimer with an oblique arrangement of the transition moments, although not favoured energetically, cannot be excluded completely. The formation of higher aggregates was also omitted here. Finally, one should keep in mind the fact that surface interactions can influence the spectral characteristics of dyes in LB films.

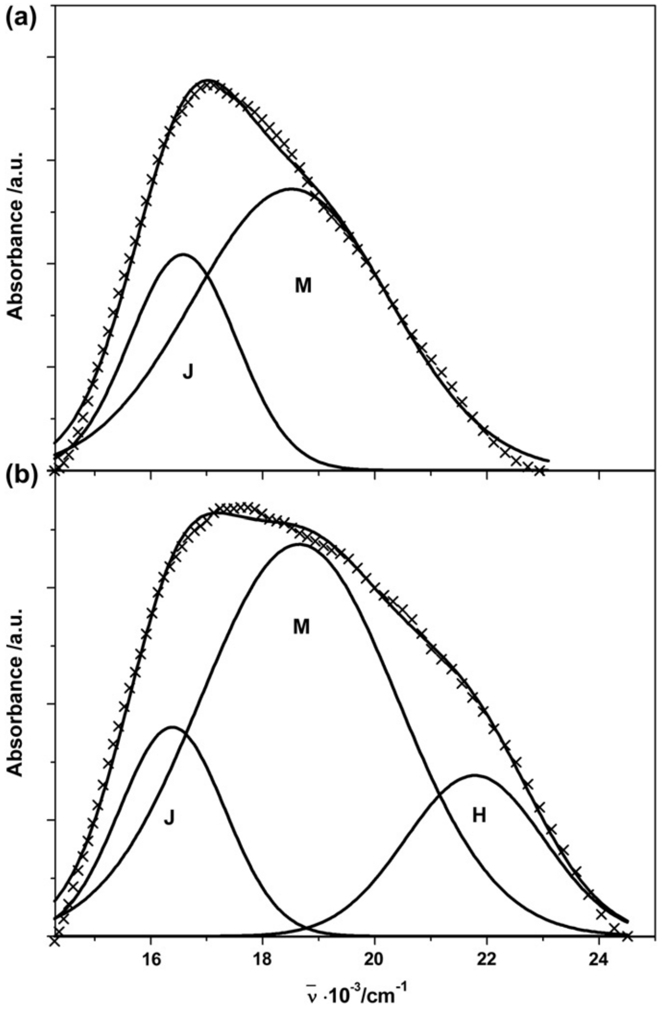

Fig. 8. Decomposition of the absorption spectrum of **4**/8CB mixture at MF = 0.1 (a) and 0.5 (b) into two (a) and three (b) Gaussian-type absorption bands.

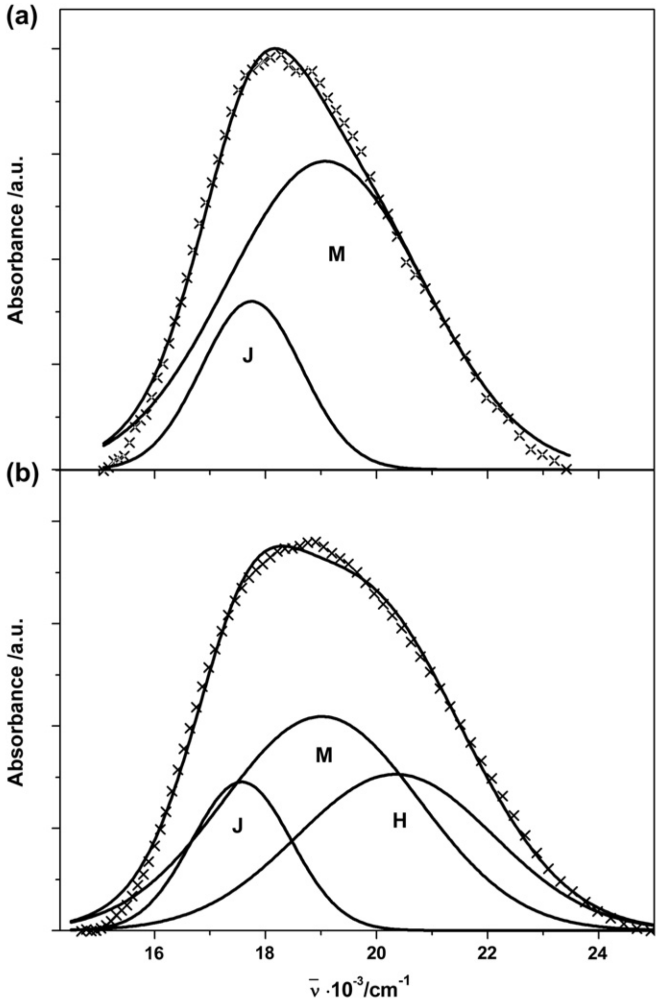

Fig. 9. Decomposition of the absorption spectrum of **2**/8PCH mixture at MF = 0.1 (a) and 0.5 (b) into two (a) and three (b) Gaussian-type absorption bands.

Nevertheless, from the analysis of the data presented in Tables 5 and 6 useful information concerning aggregate formation by the azo dyes under investigation can be obtained. In the LB films of dyes **1**, **2** and **4** mixed with both liquid

Table 5
Maximum wavenumbers of monomer and dimers bands, $\bar{\nu}_M$, $\bar{\nu}_H$ and $\bar{\nu}_J$, and ratios of band integral absorption, A_H/A_M, A_J/A_M and A_H/A_J, for azo dye/8CB mixtures resulting from the decomposition into Gaussian-type components

Dye MF	$\bar{\nu}_M$ (cm^{-1})	$\bar{\nu}_H$ (cm^{-1})	$\bar{\nu}_J$ (cm^{-1})	A_H/A_M	A_J/A_M	A_H/A_J
1						
0.1	16,950	–	15,507	–	0.15	–
0.3	16,950	18,260	15,320	0.12	0.15	0.85
0.5	16,950	18,194	15,315	0.17	0.12	1.40
0.5 (H, J)	–	16,977	15,406	–	–	4.95
2						
0.1	19,080	–	17,561	–	0.52	–
0.3	19,080	19,947	17,218	0.26	0.42	0.63
0.5	19,80	19,993	17,093	0.53	0.24	2.20
0.5 (H, J)	–	19,384	17,254	–	–	3.30
3						
0.1	19,880	–	18,947	–	2.58	
4						
0.1	18,615	–	16,579	–	0.4	–
0.2	18,615	22,146	16,344	0.19	0.69	0.27
0.3	18,615	22,186	16,425	0.20	0.50	0.42
0.4	18,615	21,769	16,323	0.37	0.58	0.64
0.5	18,615	21,391	16,563	0.43	0.43	1.00
0.5 (H, J)	–	19,685	16,721	–	–	2.35
5						
0.1	19,685	–	18,551	–	0.85	–
0.3	19,685	20,493	18,344	0.89	0.88	1.01
0.5	19,685	19,887	17,780	0.82	0.65	1.26
0.3 (H, J)	–	20,356	18,251	–	–	1.50
0.5 (H, J)	–	19,459	17,370	–	–	6.70
6						
0.1	19,342	–	18,396	–	1.10	–
0.3	19,500	20,227	17,526	0.15	0.13	1.16
0.5	19,493	21,663	17,602	0.43	1.07	0.43
0.3 (H, J)	–	19,958	17,738	–	–	2.50
0.5 (H, J)	–	19,790	16,999	–	–	3.30

Table 6
Maximum wavenumbers of monomer and dimers bands, $\bar{\nu}_M$, $\bar{\nu}_H$ and $\bar{\nu}_J$, and ratios of band integral absorption, A_H/A_M, A_J/A_M and A_H/A_J, for azo dye/8PCH mixtures resulting from the decomposition into Gaussian-type components

Dye MF	$\bar{\nu}_M$ (cm^{-1})	$\bar{\nu}_H$ (cm^{-1})	$\bar{\nu}_J$ (cm^{-1})	A_H/A_M	A_J/A_M	A_H/A_J
1						
0.1	16,950	–	15,425	–	0.15	–
0.3	16,950	18,260	15,471	0.35	0.15	2.30
0.5	16,950	18,302	15,367	0.45	0.14	3.10
0.5 (H, J)	–	17,326	15,451	–	–	9.33
2						
0.1	19,080	–	17,748	–	0.28	–
0.3	19,080	20,987	17,463	0.09	0.23	0.41
0.5	19,080	20,341	17,570	0.73	0.28	2.07
0.5 (H, J)	–	19,934	17,659	–	–	2.26
3						
0.1	19,880	–	19,309	–	0.98	–
0.3	19,880	20,748	18,796	0.07	0.12	0.57
0.5	19,880	24,839	18,981	0.68	0.37	1.85
0.3 (H, J)	–	20,462	18,792	–	–	0.42
0.5 (H, J)	–	20,729	18,571	–	–	1.29
4						
0.3	18,615	21,657	16,388	0.30	0.43	0.70
0.5	18,615	21,442	16,287	0.59	0.79	0.75
0.5 (H, J)	–	21,077	17,272	–	–	0.48
5						
0.1	19,685	–	18,685	–	0.81	–
0.3	19,685	20,660	18,055	0.27	0.26	1.02
0.5	19,685	21,313	17,363	0.74	0.16	4.50
0.3 (H, J)	–	20,297	18,207	–	–	1.74
0.5 (H, J)	–	20,036	17,438	–	–	9.29
6						
0.1	19,342	–	18,492	–	0.76	–
0.3	19,342	20,016	17,761	0.33	0.15	2.23
0.5	19,342	20,011	18,080	1.31	0.29	4.58
0.3 (H, J)	–	19,733	18,297	–	–	4.49
0.5 (H, J)	–	19,131	17,602	–	–	11.20

crystals, at low concentrations, apart from monomers, J-dimers are also created. When the dye content rises, the H-dimers appear too. For these three dyes it is reasonable to assume that, at the maximal MF, e.g. 0.5, the monomers, J-dimers and H-dimers in various fractions exist in the LB film. The fraction of J-dimers decreases with increase in the dye content, and that of the H-dimers increases. This is seen distinctly for **4**/8CB mixtures at five various MFs. Dye **3** behaves differently. Indeed the relevant results for the mixtures with 8PCH only were obtained. However, from analyzing the M, H and J peaks' positions at various MFs, it seems that, at MF ≥ 0.3, the formation of J-dimers and H-dimers, without presence of monomers, should be assumed. The best fitting for the decomposition the absorption band of **3**/PCH8 mixtures, at higher concentrations, into two components was obtained and that at MF = 0.5 is shown in Fig. 10.

The occurrence of different fractions of J-dimers and H-dimers for various dyes, at the same concentration in LB films, is most certainly connected with their molecular structures. Strictly speaking it is associated with the various directions and values of the permanent dipole moment. Dyes **1**, **2** and **4** have similar values of the dipole moment, but with different directions. The value of dipole moment of dye **3** is smaller because here the $-NO_2$ group ($\mu \approx 4$ D) is replaced by $-Cl$ group ($\mu \approx 1.5$ D). Dyes **5** and **6** have no strongly polar group. Therefore, the value of the dipole moment is very small in comparison with that of dyes **1**–**4**. Here, interaction between molecules is mostly due to dispersion forces. Searching the data listed in Tables 5 and 6 and analysis of the positions of peaks'

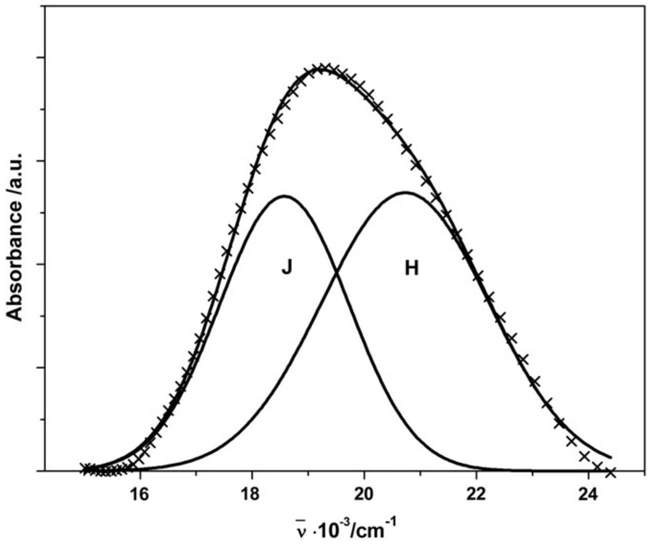

Fig. 10. Decomposition of the absorption spectrum of **3**/8PCH mixture at MF = 0.5 into two Gaussian-type absorption bands.

maxima as well as ratios of the integral absorptions, show that it is very difficult to decide if at MF ≥ 0.3 the monomers still occur or if all of the molecules form aggregates. Note that the molecular structures of dyes **5** and **6** are similar. However, the results obtained are in some cases very different. This fact confirms once more the strong effect of the dye substituent structure on the intermolecular interactions in the LB film. The influence of the type of the liquid crystal system is also seen here.

In order to evaluate quantitatively the orientation of molecules in the LB films of the azo dye/liquid crystal mixtures, polarized absorption spectra were recorded and a calculation method that is described in Refs. [5,22] was used. The average angle υ between the transition moment direction of the dye molecule in the LB film and the normal to the quartz surface was calculated from the following equation:

$$\frac{A_P}{A_S}=\frac{n_1\cos\alpha+n_3\cos\beta}{n_1\cos\beta+n_3\cos\alpha}\left(\cos\alpha\cdot\cos\beta+\frac{2n_1^3n_3\sin^2\alpha}{n_2^4\tan^2\upsilon}\right) \tag{4}$$

Here, A_P and A_S are the absorbance values at the band maximum for the light that was polarized parallelly and perpendicularly to the plane of incidence, respectively. Variable n_j are the refractive indices of the jth phases. α is the angle of incidence at the air–LB film interface, and β is the angle of refraction at the LB film–substrate interface. Here, the approximate values of $n_1 = 1$ (air), $n_2 = 1.5$ (LB film) and $n_3 = 1.49$ (quartz substrate) were used. All of the spectra for polarized light were recorded at the angle of incidence $\alpha = 0°$, 30° and 60°.

Eq. (4) is valid if the molecules in the monolayer are distributed uniformly around cone, with their transition moments tilted at an angle υ to the normal. In this case A_P/A_S for $\alpha = 0°$ should be equal to 1. On the basis of the υ angles, information concerning the orientation of molecules with respect to the slide surface can be obtained. A knowledge of the angle between the absorption oscillator and the long molecular axis of the dye is, however, necessary. In a first approximation, one can assume that the angle between the transition moment direction and the long molecular axis of dyes **1–6**, for the longwavelength absorption band, resulting from $\pi \rightarrow \pi^*$ transition, is equal to zero. Thus, the angles υ reflect directly the arrangement of dye molecules in LB films.

Figs. 11 and 12 present examples of polarized components of absorption spectra for LB films of **5**/8CB and **4**/8PCH mixtures, respectively. At $\alpha = 0°$, both components are equal. This means that the movement of the quartz slide during deposition did not disturb the homogeneity of the molecular alignment. The band occurring at .280 nm, for dye/8CB mixtures, is related to the absorption of the liquid crystal and it’s shape is the same for both components, independent of MF and α. However, the A_P and A_S for the band attributed to the dye have different shapes at MF ≥ 0.3 and $\alpha = 60°$. The same observations for mixtures of other dyes with 8CB or 8PCH were made. As the orientation of monomers and dimers can be, generally, different, the results obtained confirm the supposition that in LB films of azo dye/liquid crystal mixtures various kinds of aggregates are created.

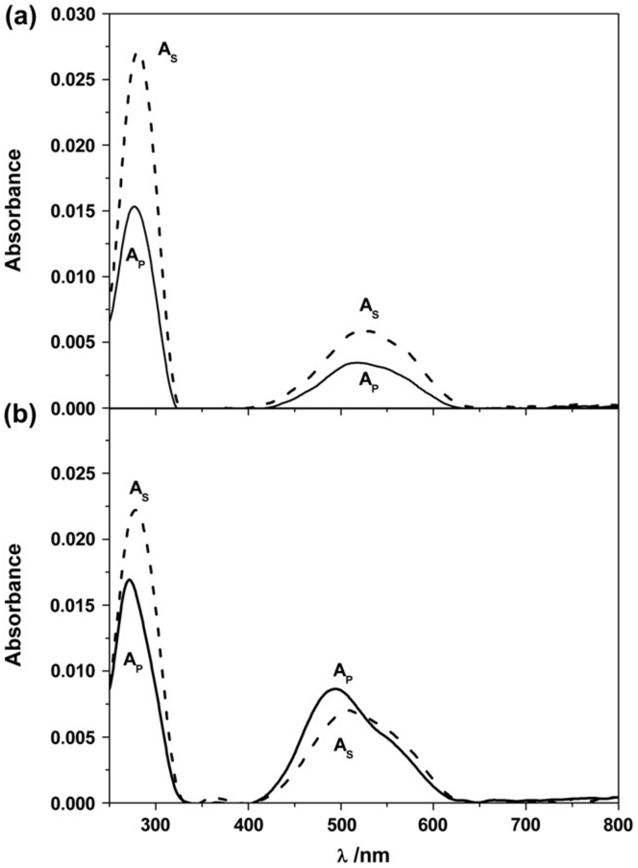

Fig. 11. Absorption spectra for light polarized parallelly (A_P) and perpendicularly (A_S) to the plane of incidence for **5**/8CB mixture as LB film at MF = 0.1 (a) and 0.3 (b). The angle of incidence was 60°.

Table 7 contains the values of the angle υ obtained for all the dye/liquid crystal mixtures investigated in LB films at MF = 0.1, 0.3 and 0.5. The values of A_P and A_S were taken at the wavelengths corresponding to the monomer, J-dimer and H-dimer peaks, given in Tables 5 and 6. These are the mean values of the results obtained at the angles of incidence, $\alpha = 30°$ and 60°, for at least three independently prepared samples. The values of υ for these two angles of incidence differ not more than 1.5°.

It follows from the results obtained that, generally, the angle υ of all the absorbed species decreases with increase in the dye content as does the angle φ in Langmuir films (see data in Tables 2 and 3). However, the value of υ for a given dye/liquid crystal mixture is greater than that of φ. This difference can be due to two reasons: (i) the molecular packing may have been deteriorated by the stress generated by the monolayer transfer from the water surface to the slide substrate and (ii) the methods used to calculate the angles υ and φ are different. The various angles between the long axis of the molecules and normal to the interface in Langmuir and LB films had been found previously for other dyes [5,23–25]. It is apparent from Table 7 that, when the dye molecules form H-dimers, their long axes show a more highly perpendicular orientation with respect to the film surface. Such an observation was made also for other compounds forming self-aggregates [5]. The greatest υ angle was obtained for J-dimers. This seems

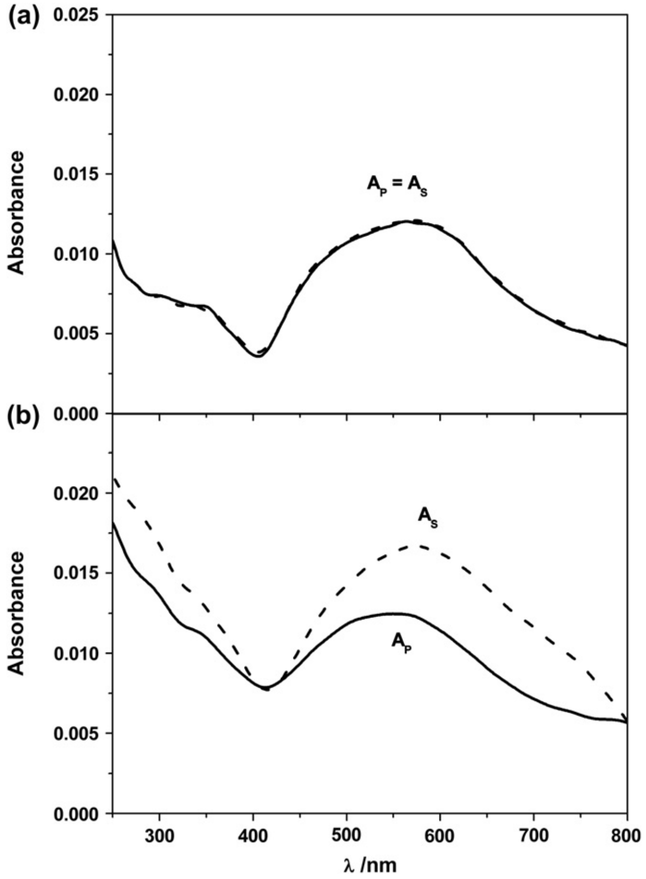

Fig. 12. Absorption spectra for light polarized parallel (A_P) and perpendicularly (A_S) to the plane of incidence for **4**/8PCH mixture as LB film at MF = 0.5. The angle of incidence was 0° (a) and 60° (b).

Table 7
Values of the angle between the molecular long axis and the normal to the quartz slide, in LB films of **1**–**6** mixed with liquid crystal

Dye MF	υ_{av} (°)					
	8CB			8PCH		
	M	H	J	M	H	J
1						
0.1	61	–	62	62	–	65
0.3	62	45	70	60	66	66
0.5	43	36	52	62	59	69
2						
0.1	43	–	47	54	–	55
0.3	43	37	53	49	34	61
0.5	41	38	49	50	37	56
3						
0.1	60	–	62	56	–	60
0.3	–	–	–	39	25	52
0.5	–	–	–	29	26	43
4						
0.1	43	–	48	–	–	–
0.3	38	45	50	69	60	70
0.5	40	37	51	62	55	78
5						
0.1	63	–	69	70	–	74
0.3	40	39	46	61	56	68
0.5	45	46	50	58	46	67
6						
0.1	43	–	43	60	–	63
0.3	33	27	39	43	25	54
0.5	36	25	40	40	23	43

to be reasonable as these dimers can be long and therefore not very rigid. One should take also into account that the transition moment direction does not need to be directed along the J-dimer long axis. It is also worth noticing that for dye **5** in 8PCH and dye **6** in both liquid crystals the υ angles for monomers and both kinds of dimers are different. Thus, it is reasonable to assume that at MF ≥ 0.3 aggregates and monomers exist in these mixtures.

The molecular orientation in LB films depends strongly on the structures of both of the dye and the liquid crystal molecules. For dyes **1**, **4** and **5**, having a lateral $-NO_2$ group (**1** and **4**) or $-OCH_3$ (**5**) group, the greatest υ values for all absorbed species were obtained, indicating that such groups can significantly loosen molecular packing during the monolayer transfer. Moreover, it is seen that, in general, in the mixtures with 8PCH, the molecules are more tilted with respect to the film surface than in corresponding mixtures with 8CB. It is possible that repulsive interactions, observed also in the Langmuir films, play some role here.

4. Conclusions

Two component Langmuir films at the air–water interface as well as Langmuir–Blodgett (LB) films on the quartz slides formed from the nonamphiphilic azo dye/liquid crystal mixtures were investigated. None of the azo dyes used that spread at the air–water interface are able to produce a stable and compressible monolayer. However, when the dyes are mixed with 8CB or with 8PCH, it is possible to obtain compressible Langmuir films on the water surface, mostly up to the MF = 0.5. The analysis of $\pi-\Sigma$ isotherms of Langmuir films reveals that the properties of the monolayer at the air–water interface (packing density, stability and rigidity) depend strongly on the structures of both the dye and the liquid crystal molecules as well as on the mixtures' composition. A characteristic is the dye concentration equivalent to the MF = 0.4. At such a content the dye is able to ‘‘stiffen’’ the liquid crystal molecules, that are tilted at a very large angle with respect to the normal to the water surface. The Langmuir films are therefore not very stable. Variation of the surface pressure at the collapse point (π_C), with the mixture composition and deviation of the average molecular area from the additivity rule indicates that the dye/liquid crystal systems that were investigated are at least partially miscible. In the most cases the negative value of the excess area (Σ_E) is observed. This suggests the predominance of the attractive interactions among the molecules. For some dyes in 8PCH, however, repulsive interactions dominate, indicating greater role of the molecular structures of both components on intermolecular interactions. Except for the **3**/8CB mixture, all other mixtures up to MF = 0.5 were transferred onto quartz slide making LB films.

The absorption spectra of azo dye/liquid crystal mixtures at MF values of dye from 10^{-3} to 0.5 were recorded. At concentrations up to MF ≈ 0.01 (measurements in a sandwich cell) no signs of aggregation were observed. Meanwhile, the absorption spectra of LB films, already at MF = 0.1, undergo very modest changes in appearance primarily in the form of a broadening of the spectrum towards the red region. The amount of the wavelength shift depends on the degree of aggregation, which is determined by the mutual orientation and the aggregation number of molecules. In analyzing the position of absorption band peak position, as well as its half-bandwidth, one can suppose that, at low concentrations, mostly J-type aggregates are formed, whereas at higher concentrations H-type aggregates dominate.

The angle between the long molecular axis of the azo dyes under investigation and the normal to the solid surface, υ, is different from the angle φ formed with the normal to the air–water interface. Although both angles are calculated from various methods, it seems that, in general, for given dye/liquid crystal mixture $\upsilon > \varphi$. This implies that the molecular packing is loosened during the monolayer transfer. However, some tendency of υ angle decrease in H-type aggregates and increase in J-type aggregates with respect to υ of the monomers can be seen. This would suggest that only aggregates in which the transition moments are aligned at high angles (>54.7°–90°) to their line of centre are able to improve the molecular packing in the LB film.

Acknowledgements

This work was supported by Research Project No. N202 080 31/306, coordinated by Ministry of Science and Higher Education.

References

[1] Roberts G. Langmuir-Blodgett films. New York: Plenum Press; 1990.

[2] Ulman A. An introduction to ultrathin organic films-from Langmuir-Blodgett to self-assembly. New York: Academic Press; 1991.

[3] Petty MC. Langmuir-Blodgett films-an introduction. Cambridge: Cambridge University Press; 1996.

[4] Reineker P, Haken H, Wold HC, editors. Organic molecular aggregates: electronic excitation and interaction processes. Berlin: Springer; 1983.

[5] Kawai T, Umemura J, Takenaka T. UV absorption spectra of azobenzene-containing long-chain fatty acids and their barium salts in spread monolayers and Langmuir-Blodgett films. Langmuir 1989;5:1378–83.

[6] Martyński T, Miyake J. Langmuir-Blodgett films of dichroic dyes oriented by liquid crystal. Supramol Sci 1998;5:643–7.

[7] Mc Ardle CB, editor. Side-chain liquid crystal polymers. Glasgow: Blackie; 1984.

[8] Martyński T, Biadasz A, Bauman D. Alignment of liquid crystal and dichroic dye molecules in mixed Langmuir and Langmuir-Blodgett films. Liq Cryst 2002;29:281–8.

[9] Bauman D, Inglot K, Martyński T, Intermolecular interactions in Langmuir and Langmuir-Blodgett films of azo dye/liquid crystal mixtures. Mol Cryst Liq Cryst, in press.

[10] Xue J, Jung CS, Kim MW. Phase transitions of liquid crystal films on an air-water interface. Phys Rev Lett 1992;69:474–7.

[11] Friedenberg MC, Fuller GG, Frank C, Robertson CR. Formation of bilayer discs and two-dimensional foams on a collapse/expanding liquid crystal monolayer. Langmuir 1994;10:1251–6.

[12] Martyński T, Hertmanowski R, Bauman D. Molecular organization in two dimensional films of liquid crystalline mixtures. III. Langmuir films of binary mixtures of liquid crystal materials with terminal –CN or –NCS group. Liq Cryst 2002;29:99–105.

[13] Inglot K, Martyński T, Bauman D. Influence of the alkyl chain length of some mesogenic molecules on the Langmuir film formation ability. Liq Cryst 2006;33:855–64.

[14] Martyński T, Hertmanowski R, Bauman D. Molecular organization in two dimensional films of liquid crystalline mixtures. I. Langmuir films of binary mixtures of liquid crystals with terminal cyano-group. Liq Cryst 2001;28:437–44.

[15] Biadasz A, Martyński T, Stolarski R, Bauman D. Molecular organization in binary mixtures of derivatives of naphthalenebicarboxylic acid and naphthoylenebenzimidazole with a liquid crystal in two-dimensional layers. I. Langmuir films. Liq Cryst 2004;31:1639–48.

[16] Gaines GL. Insoluble monolayers at liquid-gas interface. New York: Interscience; 1996.

[17] Angelova A, van der Auweraer M, Ionov R, Vollhardt D, de Schryver FC. Miscibility of alkanoic and ω-anthrylalkanoic acids in monolayers at the air/water interface studied by means of Brewster angle microscopy. Langmuir 1995;11:3167–76.

[18] Kasha M, Rawls HR, Ashraf El-Bayoumi M. The exciton in molecular spectroscopy. Pure Appl Chem 1965;11:371–92.

[19] Davydov AS. Theory of molecular excitons. New York: Mc Graw-Hill Book Company, Inc.; 1962.

[20] Moebius D. Scheibe aggregates. Adv Mater 1995;5:437–44.

[21] Miyata A, Heard D, Unuma Y, Higashigaki Y. Three types of aggregates of spiropyran with long and short hydrophobic alkyl chain. Thin Solid Films 1992;210/211:175–7.

[22] Chollet RA. Determination by infrared absorption of the orientation of molecules in monomolecular layers. Thin Solid Films 1978;52: 343–60.

[23] Johnson E, Aroca R, Nagao Y. Electronic and vibrational spectra of films and Langmuir-Blodgett monolayers of *n*-octyl-3,4-perylenedicarboximide. J Phys Chem 1991;95:8840–3.

[24] Hertmanowski R, Martyński T, Bauman D. Alignment of molecules in Langmuir and Langmuir-Blodgett films of binary mixtures of 3,4,9,10-tetra-(*n*-alkoxy-carbonyl)-perylenes with a liquid crystal. J Mol Struct 2005;741:201–11.

[25] Biadasz A, Martyński T, Stolarski R, Bauman D. Molecular organization in binary mixtures of derivatives of naphthalenebicarboxylic acid and naphthoylenebenzimidazole with a liquid crystal in two-dimensional layers. II. Langmuir-Blodgett films. Liq Cryst 2006;33: 307–19.